Carbohydrate Polymers 78 (2009) 717–724

Contents lists available at ScienceDirect

Carbohydrate Polymers

journal homepage: www.elsevier.com/locate/carbpol

Effect of cross-linker and cross-linker concentration on porosity, surface morphology and thermal behavior of metal alginates prepared from algae (*Undaria pinnatifida*)

Tara Sankar Pathak [a], Jung-Ho Yun [a], Se-Jong Lee [b], Dae-Jin Baek [c], Ki-Jung Paeng [a,*]

[a] Department of Chemistry, Yonsei University, Wonju 220-710, South Korea
[b] Department of Materials Engineering, Kyungsung University, Busan 608–736, South Korea
[c] Department of Chemistry, Hanseo University, Seosan 352-820, South Korea

ARTICLE INFO

Article history:
Received 14 April 2009
Received in revised form 8 June 2009
Accepted 9 June 2009
Available online 16 June 2009

Keywords:
Algae
Metal alginates
Scanning electron microscopy (SEM)
Porosity
Thermal degradation
Kinetics

ABSTRACT

Alginic acid and metal alginates are prepared from fresh algae using extraction method. FTIR spectra indicate that alginic acid is converted into metal alginate. Asymmetric stretching of free carboxyl group of zinc alginate at 1596 cm^{-1} is shifted to 1582 cm^{-1} in cadmium alginate, due to the change of charge density, radius and atomic weight of the cation. Surface morphology changes by changing the cross-linker and cross-linker concentration at same magnification. Total intrusion volume, porosity (%) and pore size distribution also changes by changing cross-linker and cross-linker concentration. Thermal degradation results reveals that zinc and cadmium alginates started decomposing at 100 °C, but rapid degradation started around 300 °C and showed a stepwise weight loss during thermal sweep, indicating different types of reactions during degradation. Kinetic analysis was performed to fit with TGA data, where the entire degradation process has been considered as two or three consecutive 1st order reactions.

1. Introduction

Alginate is a biopolymer extracted from algae. Naturally occurring biopolymers like alginate have been known to exhibit excellent adsorption ability for metal ions (Abu Al-Rub, El Naas, Benyahia, & Ashour, 2004; Aksu, Eretli, & Kutsal, 1998; Arica, Bayramolu, Yılmaz, Bekta, & Genc, 2004; Chen, Tendeyong, & Yiacoumi, 1997; Gotoh, Matsushima, & Kikuchi, 2004; Konoshi, Asai, Midoh, & Oku, 1993; Mimura, Ohta, Akiba, & Onodera, 2001; Muzzarelli, 1973; Pandey, Bera, Shukla, & Ray, 2007). Sodium alginate is the sodium salt of alginic acid which is a linear copolymer of 1,4-linked mannopyranosyluronic acid and 1,4-linked gulopyranosyluronic acid units.

Heavy or toxic metals such as mercury, lead, nickel, zinc, arsenic, cadmium etc. are stable trace elements which cannot be metabolized by the body and bio-accumulate in soft tissues (and bone), passing up the food chain to humans. Alginates have ability to bind heavy metals, such as mercury, lead, copper, cadmium and zinc (Carr, Harrison, Humphreys, & Sutton, 1968; Davis, Volesky, & Mucci, 2003; Korotaev et al., 1992; Sutton, Humphreys, Shepherd, & Howells, 1972).

Gelation of alginate is possible by interaction of carboxylate groups with divalent ions (Gombotz & Wee, 1998). Calcium cations are commonly used to cross-link sodium alginate. They have been reported to bind preferentially to the poly-guluronic acid units (GG) of alginate in a planar two-dimensional manner, producing the so-called "egg-box" structure (Chan, Jin, & Heng, 2002; Chan, Lee, & Heng, 2002). Alginates are very much important, due to their biodegradability, immunogenicity and ability to form gel with a variety of cross-linking agent (Lee, Sookim, & Dokim, 2005; Roy, Bajpai, & Bajpai, 2009; Suckow et al., 2000). These gels are used in various fields like food industry, medicine and biotechnological applications including cell encapsulation and drug delivery (Kierstan & Bucke, 1977; Kneafsey, Shaughnessy, & Condon, 1996).

Metal ions like Zinc and calcium cations have been reported to bind at different sites of the alginate molecule (McDowell, 1978). Aslani and Kennedy reported that zinc alginate beads release the entrapped water soluble drug paracetamol more slowly than calcium alginate beads, due to greater cross-linking by zinc ions (Aslani & Kennedy, 1996). A study compared the effects of calcium and zinc containing alginates and non-alginate dressing on blood coagulation and platelet activation to determine which was the best haemostat. The study showed that alginate materials activated coagulation more than non-alginate materials. The extent of coagulation activation was affected differently by the alginate

* Corresponding author. Tel.: +82 33 760 2239; fax: +82 33 760 2182.
E-mail address: paengk@yonsei.ac.kr (K.-J. Paeng).

0144-8617/$ - see front matter © 2009 Elsevier Ltd. All rights reserved.
doi:10.1016/j.carbpol.2009.06.011

mannuronic (M) or guluronic (G) group composition. It was demonstrated that alginates containing zinc ions had the greatest potentiating effect on prothrombotic coagulation and platelet activation (Segal, Hunt, & Gilding, 1998).

Industrial wastewater often contains toxic heavy metal ions such as zinc and cadmium at low and high concentration, and should be removed from wastewater before disposal since they are highly toxic even at low concentrations. Due to low cost and biodegradable nature of alginate, it is used as a potential adsorbent for the removal of toxic heavy metal ions like zinc and cadmium at low and high concentration. Degradation of metal (zinc and cadmium) alginates is also very much important because of environmental concern. Different metal ions (zinc and cadmium) with varying ion concentration usually affect the porosity, morphology, stability, etc.; which are also responsible for the degradation trend of corresponding metal alginates. Thus, we have observed the effect of cross-linker and cross-linker concentration on porosity, surface morphology and thermal behavior of metal alginates prepared from algae (*Undaria pinnatifida*) in the present work. The kinetic analysis was also studied to fit thermogravimetric data by considering the whole process as two or three consecutive 1st order reactions.

2. Experimental

2.1. Materials used

Dried algae {*U.* pinnatifida (Sea mustard), a kind of brown seaweeds, Avarage molecular weight; 320 kDa, determined by viscometric methods, M/G ratio; 2.1} were supplied from Kyungsung University, Busan (South Korea). Here, average molecular weight of alginate in algae is considered and determined using viscometric method. Alginate is a salt of alginic acid which is a linear polysaccharides containing 1,4-linked β-D-mannuronic (M) and α-L-guluronic (G) acid. M/G ratio means the ratio of β-D-mannuronic acid (M) and α-L-guluronic acid (G). A high performance liquid chromatography (HPLC) method reported previously (Sanchez-Machado, Lopez-Cervantes, Lopez-Hernandez, Paseiro-Losada, & Simal-Lozano, 2004) was used for the determination of the ratio of β-D-mannuronic acid and α-L-guluronic acid (M/G ratio). Sodium carbonate and cross-linker (zinc sulphate heptahydrate and cadmium sulphate hydrate) were obtained from Aldrich chemicals.

2.2. Preparation procedure of divalent metal alginates

Alginates were isolated from the algae in sodium form. Algae were processed at three principal regimes: (a) "cold" method, (b) "hot" method and (c) modified method including extraction in boiling state. Here, we used hot method for the extraction of alginate from algae. The extraction methods of alginate as well as preparation procedure of divalent metal alginates are given below.

The dried algae 2 g was stirred with an alkali solution 1.5 wt.% (sodium carbonate) for about 2 h at 50–60 °C. Alginate dissolves as sodium alginate to give very thick slurry (Pathak, Kim, Lee, Baek, & Paeng, 2008). This slurry also contains the part of the seaweed that does not dissolve, mainly cellulose. This insoluble residue removed from the solution by filtration. Sodium alginate is purified using solvent (water) and non-solvent (ethanol) method. The ratio of water and ethanol has been taken as 1:4 (v/v) in our experiment. Sodium alginate solution at a concentration of 1 wt.% was prepared by dissolving the appropriate amount of sodium alginate in ultrapure water under magnetic stirring.

Sodium alginate solution is added drop wise to metal sulphate (MSO_4; M = Zn and Cd) solution taken in a wide mouth glass jar to form divalent metal alginates. Metal alginates were taken out of solution and washed with distilled water thoroughly to remove excess metal sulphate. After washing, metal alginates were air dried. The stoichiometric reaction between sodium alginate and metal sulphate is written as:

$$2\mathrm{AlgCOONa} + \mathrm{MSO_4} \rightarrow (\mathrm{AlgCOO})_2\mathrm{M} + \mathrm{Na_2SO_4}$$

The composition of metal alginates prepared by varying cross-linker and cross-linker concentration is presented in Table 1.

2.3. Preparation of alginic acid

The sodium alginate extract is treated with dilute mineral acid, HCl at room temperature and a gelatinous precipitate of alginic acid forms which cannot be filtered; it simply blocks any filter medium. It can be removed from the liquid by flotation. The detailed preparation procedure of alginic acid is also reported in our previous study (Pathak et al., 2008).

2.4. FTIR spectra of alginic acid and metal alginates

Samples of alginic acid and metal alginates were dried first and then ground before performing FTIR analysis. FTIR spectra were recorded on a Perkin-Elmer Spectrometer. The spectra were collected from 2000 to 800 cm^{-1} range in the transmission mode with 4 cm^{-1} resolution over 40 scans.

2.5. Scanning electron microscopy (SEM)

The surface properties of metal alginates were studied using SEM. Specimen preparation was performed as follows: the dried sample was mounted on stubs and sputter-coated with gold. Micrographs were taken on a SEM instrument (Hitachi, S-4100).

2.6. Porosity

Metal alginates samples were air dried before porosity measurement. Pore diameter distribution, total intrusion volume and porosity were measured using auto pore IV 9500 V1.05 (Micromeritics Instrument Corporation, Norcross, GA, USA). Mercury filling pressure (1.33 psia) and equilibration time (10 s) was used in this study.

2.7. Thermogravimetric analysis (TGA)

Samples of metal alginates were air dried before doing TG analysis. Thermal analyses of samples were performed in the Universal V4.1D apparatus by heating up them from 18 to 800 °C with a heating rate of 10 °C/min under nitrogen atmosphere.

Table 1
Composition of metal alginates.

Sample name	Nalg, 1 wt.% (mL)	Zinc sulphate hepta hydrate (wt.%)	Cadmium sulphate hydrate (wt.%)
Znlg0.6	10	0.6	–
Znlg2	10	2	
Znlg6.25	10	6.25	–
Cdlg0.6	10	–	0.6
Cdlg2	10		2
Cdlg6.25	10	–	6.25

Nalg, sodium alginate; cross-linker, zinc sulphate heptahydrate and cadmium sulphate hydrate; cross-linker concentration, 0.6, 2 and 6.25 wt%.
Znlg, zinc alginate; Cdlg, cadmium alginate.

3. Results and discussion

Alginic acid is a linear polysaccharides containing 1,4-linked β-D-mannuronic (M) and α-L-guluronic (G) acid residues arranged in a block-wise, non-regular order along the chain (Chan, Jin, et al., 2002; Chan, Lee, et al., 2002; Chanda, Hirst, Percival, & Ross, 1952). It contains three different functional groups: —COO^- (carboxylate), —C—O—C— (ether) and —OH (alcohol). Alginates are able to adopt an ordered solution conformation through dimerization of the poly-G sequences in the presence of Ca^{2+} or other divalent cations, and this description is known as the "egg-box" model (Zheng, 1997). According to Grant et al., the egg-box model is generally invoked to explain how the divalent metal ions, bounded in the interchain cavities, essentially polyguluronate sequences, give rise to a rod-like cross-link complex (Grant, Morris, Rees, Smith, & Thom, 1973; Morris, Rees, Thom, & Boyd, 1978). The association of polyguluronate sequences by chelation of metal ion, the egg-box model is given by Rees DA and Welsh EJ (Rees & welsh, 1977); in which oxygen atoms coordinated to metal ion were shown as filled circle. When drops of sodium alginate solution get into a divalent metal sulphate solution, beads of metal alginate are immediately formed at high concentration of cross-linker solution whereas at low concentration of cross-linker, bead formation does not occur.

Kohn and Furda proposed three main factors for understanding the binding of metal cations by these polyguluronates, namely the geometry of ligand, the separation between unit charges on the chain and when chain-association is part of the binding process, the ease with which the polysaccharide chains can pack (Kohn & Furda, 1968).

The loss of weight of the bead during drying was found to be 90–92%. It was calculated using the following formula:

$$\%\ \text{Weight loss} = [(W_1 - W_2)/W_1 * 100],$$

where W_1 and W_2 are the weight of the bead before and after drying, respectively.

Polona et al. reported that wet calcium alginate bead had smooth surface and spherical shape whereas dried bead had rough surface (Polona, Marija, Anamarija, Odon, & Ales, 2007). Metal (zinc and cadmium) alginates in wet and dry state had shown same observation in our study also.

Ionic bonding between carboxylate groups of the sodium alginate with Zn^{2+} or Cd^{2+} ions results in the formation of mechanically stable networks. Similar work had been mentioned by Lee et al., who had reported similar results for the ionic bonding between carboxylate groups of the sodium alginate with Ca^{2+} ions (Lee et al., 2000).

3.1. Fourier transform infrared spectroscopy

The stretching of C=O of protonated carboxylic group of alginic acid occurs at 1730 and 1609 cm^{-1}, respectively as it is seen in Fig. 1. It is also observed that, when the proton is displaced by a monovalent ion (sodium), the peaks appear at 1601 and 1432 cm^{-1}, respectively. These peaks are assigned for asymmetric and symmetric stretching vibration of free carboxyl group of sodium alginate. In the FTIR spectrum of alginic acid (Jeon, Nah, & Hwang, 2007), the peaks around 1030 cm^{-1} are attributed to the stretching of C—O—C.

It is also observed in Fig. 1 that the peak at 1609 cm^{-1} for protonated carboxylic acid of alginic acid is shifted to the lower side when proton is displaced by divalent ion (zinc and cadmium). As divalent metal ions replace sodium ions in the sodium alginate, the charge density, the radius and the atomic weight of the cation are changed, creating a new environment around the carbonyl group. Hence, a peak shift should be expected.

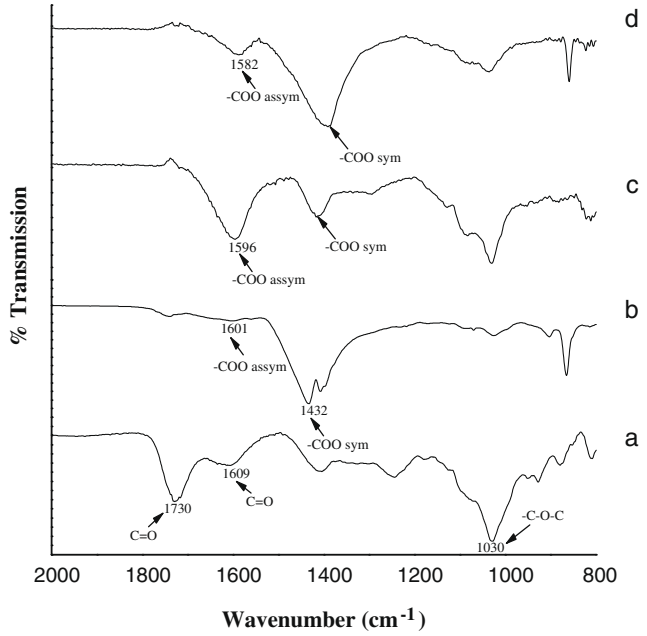

Fig. 1. FTIR spectra of (a) alginic acid, (b) sodium alginate, (c) Znlg6.25 and (d) Cdlg6.25.

The alginate have carboxylate group which played an important role in binding metal ions.

The percentage of ionic binding (PIB) can be calculated from the following formula (Chen, Hong, Wu, & Wang, 2002):

$$\text{PIB} = \left[\nu_{(\text{COOH})} - \nu_{(\text{COOM})}\right] / \left[\nu_{(\text{COOH})} - \nu_{(\text{COONa})}\right]$$

where ν is the frequency of asymmetric vibration of carboxylate group.

The denominator in the formula of PIB is the IR frequency shift of the asymmetric C=O vibration from the typical covelent bonding (carboxylic acid) to the typical ionic binding (sodium carboxylate), whereas its numerator term is the frequency shift of same vibration when a particular metal ion is bound.

PIB was calculated on the basis of the frequencies obtained from FTIR analysis (Fig. 1). The values of frequencies of $\nu_{(\text{COOH})}$, $\nu_{(\text{COONa})}$, $\nu_{(\text{COOZn})}$ and $\nu_{(\text{COOCd})}$ are 1730, 1601, 1596 and 1582 cm^{-1}, respectively.

The PIB values of Znlg6.25 and Cdlg6.25 calculated using above formula are 1.04 and 1.15. The PIB values of Znlg6.25 and Cdlg6.25 are greater than unity, due to lower metal carboxylate vibration frequencies compared to Na carboxylate. This can be interpreted as a decrease in the electron density at the carboxylate group as a result of electron delocalization. The electron delocalization could be attributed to polarization or electron feedback bonding between a metal ion and caboxylate group. In general, the electron delocalization effect is beneficial to the metal caboxylate binding (Chen et al., 2002).

3.2. Scanning electron microscopy

SEM was employed to determine the surface properties of metal alginates by varying cross-linker and cross-linker concentration. The surface morphology of zinc and cadmium alginate at 0.6, 2 and 6.25 wt.% of cross-linker concentration at fixed magnification are given in Fig. 2. SEM analysis revealed that surface morphology of metal alginates changes by changing the cross-linker and cross-linker concentration at same magnification. From SEM, we can say that zinc alginate is more porous compared to cadmium alginate at particular cross-linker concentration.

3.3. Porosity

Porosity and pore structure are very much important for the application of metal alginates in various fields. This can give a wide variety of pore diameters varying from a few nano meters to several hundred nano meters. The total intrusion volume and porosity (%) of zinc and cadmium alginate by varying cross-linker concentration are given in Table 2. It is observed in Table 2 that the total intrusion volume as well as porosity% of zinc alginate is much higher compared to cadmium alginate at particular cross-linker concentration. This can be explained on the basis of the ionic size of the cation. Sing et al. reported that comparing barium and calcium ion, barium ions fill a larger space between the alginate molecules producing a tight arrangement of the film resulting in smaller voids whereas smaller size of calcium is responsible for less tight structure on the surface with higher voids (Singh, Singh, & Kushwaha, 2007). Alginate is an anionic polysaccharide and it is preferred to bind cations of large ionic radii (Angyal, 1989). In our study, cadmium has a radius of 97 pm compared to 74 pm for zinc. So, cadmium ions are expected to fill a larger space between the alginate molecules producing a tight arrangement at the surface with smaller voids, producing a lower intrusion volume. On the other hand, zinc cations are small compared to cadmium, producing a less tight arrangement at the surface with higher voids, resulting a higher intrusion volume.

In case of zinc alginate, the total intrusion volume as well as porosity% at higher concentration is lower compared to at lower concentration of cross-linker as it is seen in Table 2, due to more packed arrangement of alginate molecule at higher concentration of cross-linker. The total intrusion volume of cadmium alginate decreases with the increase of cross-linker concentration, due to more packed arrangement of alginate molecule at higher concentration of cross-linker concentration as it is seen in Table 2 whereas porosity% of cadmium alginate didn't vary in a regular manner with the increase of cross-linker concentration.

A plot of pore size distribution (log differential intrusion against pore diameter) of zinc and cadmium alginate is given in Fig. 3. We can say from Fig. 3 that pore size distribution changes by changing the metal ion as well as cross-linker concentration.

3.4. Thermogravimetric analysis (TGA)

Thermogravimetric analysis (TGA) is one of the easiest methods to analyze thermal decompositions and kinetics of degradation process for solid materials, like coal, biomass and biopolymers. Moreover, it can provide a fast preliminary evaluation of the degradation pattern and the thermal stability of polymers with a very small amount of sample. Table 3 is presenting the weight loss percentage value at different temperatures calculated from TGA curves for zinc and cadmium alginates using the metal ion solutions of different concentrations to evaluate the exact variation in degradation trend of alginates with change in the metal ion concentrations. It can be seen that initial degradation of zinc and cadmium both the alginates took place at 100 °C, but rapid degradation started around 300 °C. It is seen from the results that, both metal alginates had degraded in various steps, indicating different types of reactions during thermal sweeps. All the cadmium alginate samples have followed similar degradation trend having three steps in their thermograms. Initial weight loss (around 100 °C) from alginates may be due to the physical loss of moisture

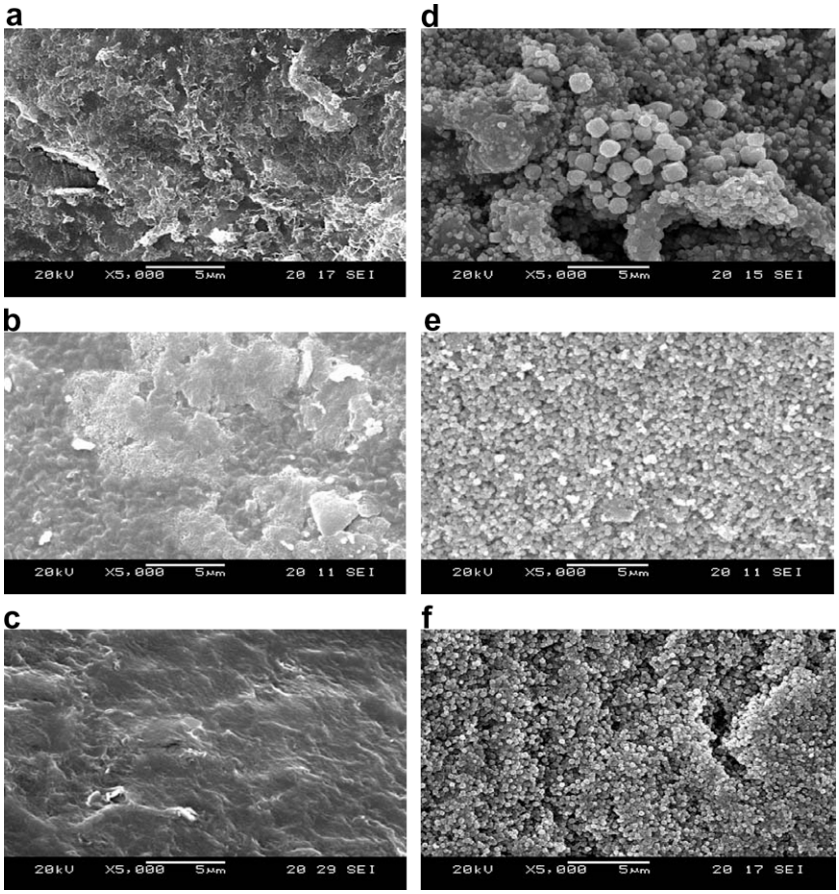

Fig. 2. Surface morphology of (a) Znlg0.6, (b) Znlg2, (c) Znlg6.25, (d) Cdlg0.6, (e) Cdlg2 and (f) Cdlg6.25 at 5000 magnification.

Table 2
Pore characteristics of metal alginates.

Sample name	Total intrusion volume (mL/g)	Bulk density (g/mL)	Apparent density (g/mL)	Porosity (%)
Znlg0.6	0.1962 ± 0.0040	2.1947 ± 0.0439	3.8539 ± 0.0771	43.05230 ± 0.00015
Znlg2	0.1152 ± 0.0028	0.6639 ± 0.0159	0.7189 ± 0.0159	7.65060 ± 0.00220
Znlg6.25	0.0684 ± 0.0015	0.6507 ± 0.0143	0.6810 ± 0.0149	4.449500 ± 0.00920
Cdlg0.6	0.1052 ± 0.0026	1.9725 ± 0.0493	2.4891 ± 0.0622	20.75445 ± 0.00035
Cdlg2	0.0557 ± 0.0012	0.1191 ± 0.0034	0.1198 ± 0.0035	0.58235 ± 0.06645
Cdlg6.25	0.0226 ± 0.0006	1.0688 ± 0.0288	1.0953 ± 0.0296	2.60195 ± 0.00275

Standard deviation value is written with ± mark.

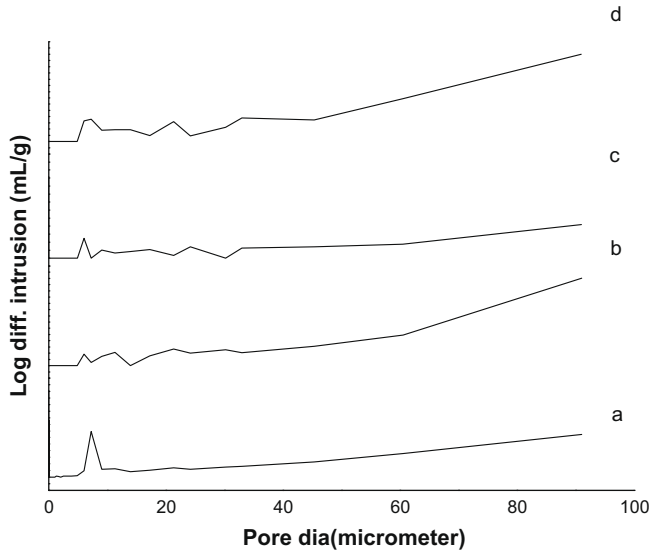

Fig. 3. Plot of log diff. intrusion (mL/g) vs. pore dia (micrometer) of (a) Znlg0.6, (b) Znlg6.25, (c) Cdlg0.6 and (d) Cdlg6.25.

from the samples. First step of rapid degradation was situated around 300–430 °C, resulting in the biopolymer degradation during this step. The final step of thermograms was appeared around 430–630 °C, which may be attributed to the cadmium carbonate formation. It is particularly noticed that, cadmium alginate becomes thermally more stable around 300–600 °C with increase in the metal ion concentration. TG analysis had further performed up to 1000 °C for Cdlg2 sample. It is seen from this thermogram that, alginate sample has degraded in negligible amount after 630 °C. Thus, from the overall results of thermal degradation, it can be concluded that trend of the thermal degradation has not much been changed for cadmium alginate with change in the metal ion concentration. On the other hand, degradation trend of zinc alginate was varied significantly with change in the Zn ion concentration. Initial weight loss around 100–150 °C has also been seen in this case, due to the physical water loss from the sample. The biopolymer degradation was performed in two steps, in between 180–305 °C and 305–650 °C; whereas the third step of decomposition was situated around 650–800 °C during the metal carbonate formation. It is worth noticing that, Znlg0.6 has degraded in remarkable amount (42–74 wt.%) in between 700 and 800 °C, whereas Znlg2 and Znlg6.25 were not degraded in considerable amount during this temperature range. When we performed TG experiment further up to 1000 °C for Znlg2 sample, we have seen that alginate sample degraded 59–79% at 800–900 °C. Therefore, it can be said that, with increase in the Zn ion concentration the thermal stability of zinc alginate samples increased at higher temperature (800 °C); whereas at low and medium temperature range, trend followed the opposite direction. It can be explained on the basis of the complex formation. Zinc ion form outer-sphere complex with alginate whereas cadmium ion form inner-sphere complex. Outer sphere complexes are mainly electrostatic and not as strong as inner-sphere complexes. In outer-sphere complexes, the metal ion or the ligand or both generally retain their coordinated water when the complex is formed. With the increase in metal ion concentration, a thicker layer of metal ion is produced on the alginate surface. Cadmium exhibits essentially bidentate linkages with the oxygen of the carboxylate whereas zinc forms preferentially monodentate bonds with the hydroxyl group of the carboxyl ligand. The main reason for this difference is a larger size of cadmium ion, which allows the formation for Cd of stable chelate rings with oxygen-metal–oxygen angles close to 90° whereas smaller zinc ion allows the formation of unstable zinc chelates. The thermal stability of zinc alginate samples decreased with the increase in zinc ion concentration at low and medium temperature whereas thermal stability of cadmium alginate samples increased with the increase in cadmium ion concentration, due to different complexing nature of zinc and cadmium. However, complex formation nature between metal ion and functional group on the alginate surface was complicated and difficult to understand; thus thermal degradation behavior of metal alginates is not still clear to us.

3.4.1. Kinetic analysis

The integral method (Coats & Redfern, 1964) was used to calculate the kinetic parameters like, activation energy and pre-exponential factor value of thermal degradation reaction for zinc and cadmium alginate with different concentrations of corresponding

Table 3
Percent weight loss of metal alginate from TGA analysis.

Sample name	% wt. loss at different temp. (°C), heating rate = 10 °C/min									
	100	200	300	400	500	600	700	800	900	1000
Znlg0.6	6.53	11.30	31.21	37.25	39.81	40.12	42.39	74.02	n.d.	n.d.
Znlg2	4.01	15.02	36.02	47.92	53.19	53.83	54.77	58.95	79.37	86.23
Znlg6.25	5.66	17.13	37.18	46.81	52.91	54.48	55.39	56.28	n.d.	n.d.
Cdlg0.6	7.43	14.16	27.20	46.14	58.04	83.04	n.d.	n.d.	n.d.	n.d.
Cdlg2	4.47	12.18	24.97	42.77	57.59	84.32	87.73	88.53	88.72	89.13
Cdlg6.25	1.25	11.19	20.39	33.67	45.94	68.24	75.52	76.65	n.d.	n.d.

n.d., not determined.

metal ions. The thermal processes were divided into two or three suitable steps, and each step was assumed as 1st order reaction. Therefore the kinetic equation can now be written simply by the following expression for each step:

$$dx/dt = A\ \exp(-E/RT)(1-x) \quad (1)$$

In this expression A is pre-exponential factor, E is activation energy, T is temperature, t is time and x represents the mass fraction of the sample. Here, x is expressed as the following equation: $x = (W_0 - W_t)/(W_0 - W_f)$, where W_0, W_t and W_f are representing the initial weight, weight at temperature T and final weight of the test sample, respectively. At a constant heating rate H (=dT/dt) during thermal degradation Eq. (1) can be rearranged and after integration it can be written as:

$$\ln[-\ln(1-X)/T^2] = \ln\left[\frac{AR}{HE}\left(1-\frac{2RT}{E}\right)\right] - \frac{E}{RT} \quad (2)$$

In Eq. (2), the expression $\ln[\frac{AR}{HE}(1-\frac{2RT}{E})]$ is constant for the most E values and written in Eq. (2) is constant for most values of E and for the temperature range used during the thermal degradation process. Therefore, for a first order reaction a straight line should be obtained, if the left side of Eq. (2) is plotted against $1/T$. The value of slope and intercept was obtained from the graph for all alginate samples for every degradation temperature range. The value of slope ($-E/R$) is used to calculate the activation energy. Similarly, pre-exponential factor can also be calculated from the intercept value by putting the temperature at which $W_t = (W_0 + W_f)/2$ in the place of T (Chattopadhyay, Kim, Kim, & Pak, 2008; Zhou, Wang, Huang, & Cai, 2006).

Fig. 4 is showing the typical plots of $\ln[-\ln(1-x)/T^2]$ vs. $1/T$ for the zinc alginate sample (Znlg0.6) and the heating rate used in this case is 10 °C/min. Here, the entire thermal process of alginate sample (Znlg0.6) was divided into three consecutive 1st order reactions. Eq. (1) has been applied separately to each of the stages by calculating the value of x separately for each reaction, and thus essentially straight line has come in each independent step. Table 4 represents the kinetic parameters calculated for all the alginate samples for various stages at heating rate of 10 °C/min using the same method. The kinetic parameters are obtained from x = 0.06–10% to 53–86%, which is the main degradation region for all the alginate samples.

The activation energy values calculated for the thermal degradation reaction of metal alginates did not show any significant dependence on the metal ion concentrations. There are two samples, Znlg6.25 and Cdlg2 for which, the whole process was divided into two stages of 1st order reactions. For all the other alginates, it has been assumed as three consecutive 1st order reactions. If we consider E values for Znlg0.6 and Znlg2 it is seen that, 1st and 3rd stage of thermal degradation had positive value; whereas 2nd stage of reaction possessed the E value in negative. The value of E reaches at its highest point at the final stage of thermal reaction for these two samples. In Znlg6.25 degradation process was almost stop after 500 °C, thus kinetic parameters had also been calculated up to 505 °C (778 K), considering the whole process into two 1st order reactions. On the other hand, Cdlg2 had decomposed almost 86% at 889 K, and negligible amount of degradation took place above that temperature. Thus, the kinetic parameters have not been calculated further, and the process was divided into two consecutive 1st order reactions. For all the cadmium alginates, activation energy (E) is possessing positive value in every steps. In general trend, the value of E reaches at its highest point at the final stage of thermal reaction for the samples having three stages of 1st order reactions. Reaction with high activation energy requires a high temperature or a long residence time (Lazaro, Moliner, & Suel-

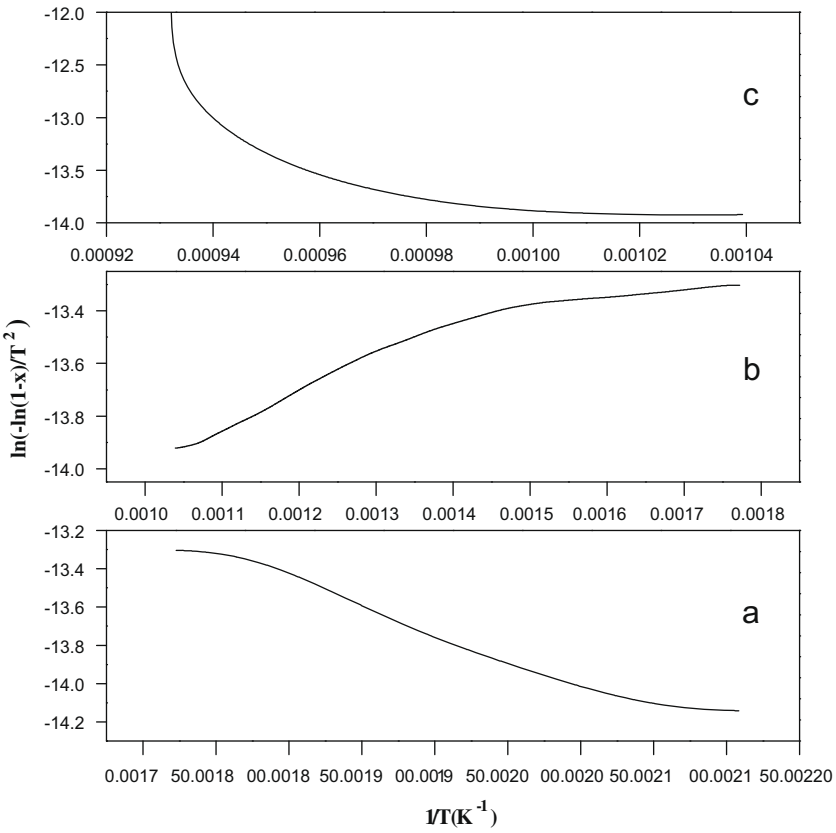

Fig. 4. Plot of $\ln[-\ln(1-X)/T^2]$ vs. $1/T$ at heating rate of 10 °C/min in the temperature range (a) 463–563 K, (b) 563–868 K and (c) 961–1073 K from TGA data for zinc alginate sample (Znlg0.6).

Table 4
Kinetics parameters of metal alginates obtained from TGA analysis.

Sample name	Heating rate (°C/min)	Temp. (K)	Conversion range (%)	E (kJ/mol)	A (min^{-1})
Znlg0.6	10	463–563	10.62–30.41	27.7	0.112
		563–961	30.41–41.79	−11.8	0.005
		961–1073	41.79–74.02	332	2.417
Znlg2	10	436–723	8.45–51.61	8.314	0.163
		723–1022	51.61–55.66	−16.6	0.009
		1022–1188	55.66–82.87	187.5	0.658
Znlg6.25	10	418–558	9.45–35.58	18.47	0.176
		558–778	35.58–53.11	9.23	1.089
Cdlg0.6	10	294–447	0.06–10.97	4.37	0.003
		447–679	10.97–47.07	23.75	0.116
		679–866	47.07–81.80	56.68	0.415
Cdlg2	10	450–686	8.97–45.67	27.7	0.124
		686–889	45.67–86.32	29.9	0.366
Cdlg6.25	10	420–556	3.85–19.31	18.4	0.101
		556–683	19.31–35.41	27.7	0.088
		683–889	35.41–71.36	66.5	0.441

ves, 1998). Usually, high activation energy means that the reaction needs more energy from the surroundings during the reaction, for thermal degradation process. In this case, Znlg0.6 sample was possessing highest activation energy value of 332 kJ/mol at the final stage of degradation process. On the other hand, the process with negative activation energy is the one in which, reaction rate decreases with increasing temperatures. Reactions exhibiting these negative E values are typically barrierless reactions.

4. Conclusions

Hot extraction method is used for the preparation of alginic acid and metal alginate from algae. FTIR spectroscopy confirmed the formation of alginic acid and metal alginates. Surface morphology changes by varying the cross-linker and cross-linker concentration at same magnification. Similarly, total intrusion volume, porosity percentage and pore size distribution had been affected with changes in the cross-linker and cross-linker concentration. Zinc and cadmium alginates had degraded in various steps and showed a stepwise weight loss during thermal sweep, indicating different types of reactions during thermal degradation. The thermal stability of zinc alginate samples decreased with the increase in zinc ion concentration at low and medium temperature whereas thermal stability of cadmium alginate samples increased with the increase in cadmium ion concentration, due to different complexing nature of zinc and cadmium. The kinetic analysis results, obtained on the basis of thermal degradation process of metal (zinc and cadmium) alginates show two or three consecutive 1st order reactions for the different subintervals of weight loss found quite satisfactorily with the Arrhenius law. Due to low cost and biodegradable nature of alginate, it is used as a potential adsorbent for the removal of toxic heavy metal ions like zinc and cadmium at low and high concentration.

Acknowledgement

This study was supported by a Grant of Korea Institute of Marine Science and Technology Promotion (KIMST), South Korea.

References

Abu Al-Rub, F. A., El Naas, M. H., Benyahia, F., & Ashour, I. (2004). Biosorption of nickel on blank alginate beads, free and immobilized algal cells. *Process Biochemistry, 39*(11), 1767–1773.

Aksu, Z., Eretli, G., & Kutsal, T. A. (1998). Comparative study of copper(II) biosorption on Ca-alginate, agarose and immobilized *C. vulgaris* in a packed-bed column. *Process Biochemistry, 33*(4), 393–400.

Angyal, S. J. (1989). Complexes of metal cations with carbohydrates in solution. *Advances in Carbohydrate Chemistry and Biochemistry, 47*, 1–43.

Arica, M. Y., Bayramolu, G., Yılmaz, M., Bekta, S., & Genc, O. (2004). Biosorption of Hg^{2+}, Cd^{2+}, and Zn^{2+} by Ca-alginate and immobilized wood-rotting fungus *Funalia trogii*. *Journal of Hazardous Material, 109*(1–3), 191–199.

Aslani, P., & Kennedy, R. A. (1996). Effect of gelation conditions and dissolution media on the release of paracetamol from alginate gel beads. *Journal of Microencapsulation, 13*(5), 601–614.

Carr, T. E., Harrison, G. E., Humphreys, E. R., & Sutton, A. (1968). Reduction in the absorption and retention of dietary strontium in man by alginate. *International Journal of Radiation Biology and Related Studies in Physics Chemistry and Medicine, 14*, 225–233.

Chan, L. W., Jin, Y., & Heng, P. W. S. (2002). Cross-linking mechanisms of calcium and zinc in production of alginate microspheres. *International Journal of Pharmaceutics, 242*(1–2), 255–258.

Chan, L. W., Lee, H. Y., & Heng, P. W. S. (2002). Production of alginate microspheres by internal gelation using an emulsification method. *International Journal of Pharmaceutics, 242*(1–2), 259–262.

Chanda, S. K., Hirst, E. L., Percival, B. G. V., & Ross, A. G. (1952). The structure of alginic acid Part II. *Journal of Chemical Society, 183*, 3–1837.

Chattopadhyay, J., Kim, C., Kim, R., & Pak, D. (2008). Thermogravimetric characteristics and kinetic study of biomass co-pyrolysis with plastics. *Korean Journal of Chemical Engineering, 25*(5), 1047–1053.

Chen, J. P., Hong, L., Wu, S., & Wang, L. (2002). Elucidation of interactions between metal ions and Ca alginate-based ion-exchange resin by spectroscopic analysis and modeling simulation. *Langmuir, 18*(24), 9413–9421.

Chen, J. P., Tendeyong, F., & Yiacoumi, S. (1997). Equilibrium and kinetic studies of copper ion uptake by calcium alginate. *Environmental Science and Technology, 31*(5), 1433–1439.

Coats, A. W., & Redfern, J. F. (1964). Kinetic parameters from thermogravimetric data. *Nature, 201*(4914), 68–69.

Davis, T. A., Volesky, B., & Mucci, A. (2003). A review of the biochemistry of heavy metal biosorption by brown algae. *Water Research, 37*, 4311–4330.

Gombotz, W., & Wee, S. W. (1998). Protein release from alginate matrices. *Advanced Drug Delivery Reviews, 31*(3), 267–285.

Gotoh, T., Matsushima, K., & Kikuchi, K. I. (2004). Adsorption of Cu and Mn on covalently cross-linked alginate gel beads. *Chemosphere, 55*(1), 57–64.

Grant, G. T., Morris, E. R., Rees, D. A., Smith, P. J. C., & Thom, D. (1973). Biological interactions between polysaccharides and divalent cations: The egg-box model. *FEBS Letters, 32*(1), 195–198.

Jeon, C., Nah, I. W., & Hwang, K. Y. (2007). Adsorption of heavy metals using magnetically modified alginic acid. *Hydrometallurgy, 86*(3–4), 140–146.

Kierstan, M., & Bucke, C. (1977). The immobilization of microbial cells, subcellular organelles, and enzymes in calcium alginate gels. *Biotechnology and Bioengineering, 19*(3), 387–397.

Kneafsey, B., Shaughnessy, M. O., & Condon, K. C. (1996). The use of calcium alginate dressings in deep hand burns. *Burns, 22*(1), 40–43.

Kohn, R., & Furda, I. (1968). Binding of calcium ions to acetyl derivatives of pectin. *Collection of Czechoslovak Chemical Communications, 33*, 2217–2225.

Konoshi, Y., Asai, S., Midoh, Y., & Oku, M. (1993). Recovery of zinc, cadmium, and lanthanum by biopolymer gel particles of alginic acid. *Separation Science and Technology, 28*(9), 1691–1702.

Korotaev, G. K., Chlenov, M. A., Kirianov, A. V., Arazashvili, A. I., Kuznetsova, E. K., Ivannikov, A. T., et al. (1992). Modified calcium alginate–a highly effective agent for eliminating radioactive strontium. *Radiobiologiia, 32*, 126–129.

Lazaro, M. J., Moliner, R., & Suelves, I. (1998). Non-isothermal versus isothermal technique to evaluate kinetic parameters of coal pyrolysis. *Journal of Analytical and Applied Pyrolysis, 47*(2), 111–125.

Lee, K. Y., Rowley, J. A., Eiselt, P., Moy, E. M., Bouhadir, K. H., & Mooney, D. J. (2000). Controlling mechanical and swelling properties of alginate hydrogels independently by cross-linker type and cross-linking density. *Macromolecules, 33*(11), 4291–4294.

Lee, Y. H., Sookim, J., & Dokim, H. (2005). A study of biodegradable superabsorbent materials based on acrylonitrile grafted sodium alginate. *Key Engineering Material, 277–279*, 450–454.

McDowell, R. H. (1978). *Properties of Alginates*. London: Alginate Industries Ltd.

Mimura, H., Ohta, H., Akiba, K., & Onodera, Y. (2001). Uptake behavior of americium on alginic acid and alginate polymer gels. *Journal of Radioanalytical and Nuclear Chemistry, 247*(1), 33–38.

Morris, E. R., Rees, D. A., Thom, D., & Boyd, J. (1978). Chiroptical and stoichiometric evidence of a specific, primary dimerisation process in alginate gelation. *Carbohydrate Research, 66*(1), 145–154.

Muzzarelli, R. A. A (1973). In Natural chelating polymers international series of monographs in analytical chemistry. Oxford, UK: Pergamon Press.

Pandey, A., Bera, D., Shukla, A., & Ray, L. (2007). Studies on Cr(VI), Pb(II) and Cu(II) adsorption–desorption using calcium alginate as biopolymer. *Chemical Separation and Bioavailability, 19*(1), 17–24.

Pathak, T. S., Kim, J. S., Lee, S. J., Baek, D. J., & Paeng, K. J. (2008). Preparation of alginic acid and metal alginate from algae and their comparative study. *Journal of Polymers and the Environment, 16*(3), 198–204.

Polona, S., Marija, B., Anamarija, Z., Odon, P., & Ales, M. (2007). Shape optimization and characterization of polysaccharide beads prepared by ionotropic gelation. *Journal of Microencapsulation, 25*(2), 90–105.

Rees, D. A., & Welsh, E. J. (1977). Secondary and tertiary structure of polysaccharides in solutions and gels. *Angewandte Chemie International Edition in English, 16*(4), 214–224.

Roy, A., Bajpai, J., & Bajpai, A. K. (2009). Dynamics of controlled release of chlorpyrifos from swelling and eroding biopolymeric microspheres of calcium alginate and starch. *Carbohydrate Polymers, 76*(2), 222–231.

Sanchez-Machado, D. I., Lopez-Cervantes, J., Lopez-Hernandez, J., Paseiro-Losada, P., & Simal-Lozano, J. (2004). Determination of the uronic acid composition of seaweed dietary fibre by HPLC. *Biomedical Chromatography, 18*, 90–97.

Segal, H. C., Hunt, B. J., & Gilding, K. (1998). The effects of alginate and non-alginate wound dressings on blood coagulation and platelet activation. *Journal of Biomaterials Application, 12*(3), 249–257.

Singh, A., Singh, D. K., & Kushwaha, V. B. (2007). Alginates as binding matrix for bio-molluscides against harmful snails lymnaea acuminate. *Journal of Applied Polymer Science, 105*(3), 1275–1279.

Suckow, M. A., Park, K., Siger, L., Turek, J., Bore, D., & Van Horn, D. (2000). Immunogenicity of antigens in boiled alginate microspheres. *Journal of Biomater Science, Polymer Edition, 11*(1), 55–68.

Sutton, A., Humphreys, E. R., Shepherd, H., & Howells, G. R. (1972). Reduction in the retention of radioactive barium in rats following the addition of sodium alginate derivatives to the diet. *International Journal of Radiation Biology and Related Studies in Physics, Chemistry and Medicine, 22*, 297–300.

Zheng, H. (1997). Interaction mechanism in sol–gel transition of alginate solutions by addition of divalent cations. *Carbohydrate Research, 302*(1–2), 97–101.

Zhou, L., Wang, Y., Huang, Q., & Cai, J. (2006). Thermogravimetric characteristics and kinetic of plastic and biomass blends co-pyrolysis. *Fuel Processing Technology, 87*(11), 963–969.